Simultaneous Tuning of Activity and Water Solubility of Complex Catalysts by Acid−Base Equilibrium of Ligands for Conversion of Carbon Dioxide

Yuichiro Himeda,* Nobuko Onozawa-Komatsuzaki, Hideki Sugihara, and Kazuyuki Kasuga

National Institute of Advanced Industrial Science and Technology, Tsukuba Central 5-2, 1-1-1 Higashi, Tsukuba, Ibaraki 305-8565, Japan

Received October 2, 2006

New strategy for the simultaneous tuning of catalytic activity and water solubility of complex catalysts is described on the basis of an acid−base equilibrium between pyridinol and pyridinolate as the catalyst ligands. Herein, half-sandwich complexes with 4,4′-dihydroxy-2,2′-bipyridine (DHBP) or 4,7-dihydroxy-1,10-phenanthroline (DHPT) served as highly efficient and recyclable catalysts for the hydrogenation of bicarbonate in water. The oxyanion generated from the phenolic hydroxy group shows strong electronic donation and polarity, which play significant roles in the catalytic activity and water solubility, respectively. As a result, turnover frequencies (TOF) up to 42 000 h^{-1} and turnover numbers (TON) up to 222 000 have been obtained by using iridium catalysts under 6 MPa at 120 °C. Furthermore, an iridium DHPT catalyst was spontaneously precipitated at the end of the reaction. Iridium leaching was found to be 0.11 ppm (1.2% of the loaded catalyst), and the added base was completely consumed. The recovered catalyst could be recycled for four cycles with high catalytic activity. Consequently, the catalyst was homogeneous and highly activated at the beginning of the reaction, whereas it was heterogeneous and deactivated at the end. The catalytic system offers an environmentally benign process with high efficiency, easy separation, catalyst recycling, waste-free process, and aqueous catalysis.

1. Introduction

In the rapidly growing area of green chemistry,[1] developments of alternative chemical processes, alternative feedstocks, and alternative solvents have received considerable attention.[2] Extensive efforts have been undertaken for optimizing the entire chemical process consisting of reaction and separation steps in order to minimize economic and environmental costs. Homogeneous catalysis, which generally has many advantages in the reaction step as compared to the heterogeneous catalysis, has recently become increasingly important for both industrial applications and new reactions. However, the considerable difficulty involved in separation of catalyst from product and/or solvent is an inherent disadvantage.[3−6] Widely used separation technique is relying on the manipulation of the reaction solvent (e.g., organic/aqueous,[7] organic/fluorous liquid,[8] or supercritical fluids/inonic liquid[9−12]). Other strategies for catalyst recycling are the design of diverse and variable ligands such as supported,[13,14] polymeric,[15] or dendritic[16,17] catalysts. Recently, substantial attention has been focused on stimuli-responsive catalysts, such as redox-switchable,[18] magnetic,[19] temperature-responsible,[20] and self-assembly supported[21] catalysts. Bullock et al. reported a self-precipitation catalyst at the end of the reaction, which helps to avoid the use of solvent and generation of waste in the subsequent separation step.[22] However, various concerns such as activity, catalyst leaching, mass transport, and environmental persistence still remain.[6] In particular, a sophisticated design mostly resulted in increasingly expensive complexes.

* To whom correspondence should be addressed. E-mail: himeda.y@aist.go.jp.

(1) Anastas, P. T.; Warner, J. C. *Green Chemistry: Theory and Practice*; Oxford University Press: New York, 1998.

(2) Poliakoff, M.; Fitzpatrick, J. M.; Farren, T. R.; Anastas, P. T. *Science* **2002**, *297*, 807−810.

(3) Baker, R. T.; Tumas, W. *Science* **1999**, *284*, 1477−1479.

(4) (a) Gladysz, J. A. *Pure Appl. Chem.* **2001**, *73*, 1319−1324. (b) Thematic Issue: Recoverable Catalysts and Reagents; Gladysz, J. A., Ed.; *Chem. Rev.* **2002**, *102*, No.10.

(5) Tzschucke, C. C.; Markert, C.; Bannwarth, W.; Roller, S.; Hebel, A.; Haag, R. *Angew. Chem. Int. Ed.* **2002**, *41*, 3964−4000.

(6) Cole-Hamilton, D. J. *Science* **2003**, *299*, 1702−1706.

(7) Cornils, B.; Herrmann, W. A. *Aqueous-Phase Organometallic Catalysis, Concepts and Applications*; Wiley-VCH: Weinheim, Germany, 1998.

(8) Horvath, I. T. *Acc. Chem. Res.* **1998**, *31*, 641−650.

(9) Blanchard, L. A.; Hancu, D.; Beckman, E. J.; Brennecke, J. F. *Nature* **1999**, *399*, 28−29.

(10) Solinas, M.; Pfaltz, A.; Cozzi, P. G.; Leitner, W. *J. Am. Chem. Soc.* **2004**, *126*, 16142−16147.

(11) Webb, P. B.; Sellin, M. F.; Kunene, T. E.; Williamson, S.; Slawin, A. M. Z.; Cole-Hamilton, D. J. *J. Am. Chem. Soc.* **2003**, *125*, 15577−15588.

(12) New solvent systems: (a) Heldebrant, D. J.; Jessop, P. G. *J. Am. Chem. Soc.* **2003**, *125*, 5600−5601. (b) Jessop, P. G.; Heldebrant, D. J.; Li, X.; Eckert, C. A.; Liotta, C. L. *Nature* **2005**, *436*, 1102. (c) Chang, D.-H.; Lee, D.-Y.; Hong, B.-S.; Choi, J.-H.; Jun, C.-H. *J. Am. Chem. Soc.* **2004**, *126*, 424−425.

(13) Hu, A.; Ngo, H. L.; Lin, W. *J. Am. Chem. Soc.* **2003**, *125*, 11490−11491.

(14) Liang, Y.; Jing, Q.; Li, X.; Shi, L.; Ding, K. *J. Am. Chem. Soc.* **2005**, *127*, 7694−7695.

(15) Li, X.; Wu, X.; Chen, W.; Hancock, F. E.; King, F.; Xiao, J. *Org. Lett.* **2004**, *6*, 3321−3324.

(16) Deng, G.-J.; Fan, Q.-H.; Chen. X.-M.; Liu, D.-S.; Chen, A. S. C. *Chem. Commun.* **2002**, 1570−1571.

(17) Dijkstra, H. P.; Van Klink, G. P. M.; Van Koten, G. *Acc. Chem. Res.* **2002**, *35*, 798−810.

(18) Subner, M.; Plenio, H. *Angew. Chem., Int. Ed.* **2005**, *44*, 6885−6888.

(19) Hu, A.; Yee, G. T.; Lin, W. *J. Am. Chem. Soc.* **2005**, *127*, 12486−12487.

(20) Wende, M.; Gladysz, J. A. *J. Am. Chem. Soc.* **2003**, *125*, 5861−5872.

(21) Yoon, J. H.; Park, Y. J.; Lee, J. H.; Yoo, J.; Jun, C.-H. *Org. Lett.* **2005**, *7*, 2889−2892.

(22) Dioumaev, V. K.; Bullock, R. M. *Nature* **2003**, *424*, 530−532.

10.1021/om060899e CCC: $37.00
Publication on Web 01/05/2007

Carbon dioxide (CO_2) is the ultimate renewable feedstock: it is highly thermodynamically stable and difficult to activate chemically.[23−26] Since the homogeneous catalysts for the hydrogenation of CO_2 were found by Inoue in 1976,[27] several groups proposed many active catalysts, mainly phosphine complexes with platinum-group metals[26,28] in supercritical CO_2[29] and in water with[30]/without[31,32] organic additives. Under ambient conditions, the reaction has been reported only by Leitner (TON of 3 per day).[30c] However, for practical applications, unsatisfactory catalytic efficiency, use of precious metal catalysts,[33] and organic additives such as amines are serious drawbacks.

Water is an innocuous, abundant, and inexpensive solvent:[7,34] it offers certain advantages such as easy separation from apolar compounds, high absorption for some gases (e.g., CO_2 under alkaline conditions), and amphoteric behavior in Brønsted sense.[35] Thus far, imparting water solubility to complexes for aqueous catalysis can be achieved by the introduction of charged or polar substituents such as anionic (SO_3H, CO_2H), cationic (NR_2), and neutral (OR) substituents into the ligands.[36] Although various phosphine ligands have been the subject of considerable research in the area of aqueous catalysts, other types of water-soluble ligands have hardly been investigated.

Table 1. Hydrogenation of CO_2 or Bicarbonate Catalyzed by [Cp*Rh(bpy)Cl]Cl 1a in Water[a]

solution	TON
H_2O	31
1 M NaH_2PO_4 aq	76
1 M KOH aq	216

[a] The reaction was carried out using a catalyst (0.2 mM) under 4 MPa (CO_2:H_2 = 1:1) at 80 °C for 20 h.

We describe a successful strategy for a novel catalyst design and catalyst tuning, which is based on the acid−base equilibrium between pyridinol and pyridinolate as the catalyst ligands. This leads to the optimization of the chemical process by tuning of the catalytic activity and water solubility, which can be attributed to the electronic effect and polarity, respectively, in both the reaction and the separation steps. As a result, a highly efficient and environmentally benign process that provides easy separation, catalyst recycling, waste-free process, and aqueous catalysis was achieved in the conversion of CO_2. In the preliminary communication, we individually reported highly efficient catalysis[37] and catalyst recycling by self-precipitation.[38] In this paper, we present both the above-mentioned subjects along with an appropriate discussion focusing on the acid−base equilibrium of the catalyst ligand. It has been confirmed that a high catalytic activity can be attributed to the strong electron-donating oxyanion on the ligand, from the result of the correlation of the catalytic activity with the Hammett constant (σ_p^+) of the substituent. The pH-dependent behavior of the complexes and a possible catalytic mechanism are discussed in detail.

2. Results and Discussion

2.1. Catalyst Design. In our previous study on the transfer hydrogenation of ketones catalyzed by half-sandwich bipyridine complexes [Cp*M(bpy)Cl]Cl (**1a**: M = Rh, **2a**: M = Ir) and [(C_6Me_6)Ru(bpy)Cl]Cl **3a** in water,[39] we also found that the decomposition of formic acid to CO_2 and H_2 proceeded smoothly using the complexes. This prompted us to investigate the reverse reaction, namely, the hydrogenation of CO_2 or bicarbonate (eq 1). In fact, rhodium complex **1a** converted CO_2

$$CO_2 + H_2 + OH^- \rightleftharpoons HCO_2^- + H_2O \qquad (1)$$

into formate under CO_2/H_2 pressure in amine-free aqueous solutions under both acidic and basic conditions (Table 1).[40] However, the catalytic activity was poor. The decomposition of formate as a reverse reaction occurred easily after the pressure release, particularly in acidic solutions. In addition, it was difficult to recover and recycle the precious platinum-group metal catalysts. In order to overcome these problems, we have designed a novel catalyst based on the bipyridine complexes.

(23) (a) Arakawa, H.; Aresta, M.; Armor, J. N.; Barteau, M. A.; Beckman, E. J.; Bell, A. T.; Bercaw, J. E.; Creutz, C.; Dinjus, E.; Dixon, D. A.; Domen, K.; DuBois, D. L.; Eckert, J.; Fujita, E.; Gibson, D. H.; Goddard, W. A.; Goodman, W.; Keller, J.; Kubas, G. J.; Kung, H. H.; Lyons, J. E.; Manzer, L. E.; Marks, T. J.; Morokuma, K.; Nicholas, K. M.; Periana, R.; Que, L.; Rostrup-Nielson, J.; Sachtler, W. M. H.; Schmidt, L. D.; Sen, A.; Somorjai, G. A.; Stair, P.; Stults, B. R.; Tumas, W. *Chem. Rev.* **2001**, *101*, 953−99. (b) Song, C.; Gaffney, A. F.; Fujimoto, K., Eds. *CO_2 Conversion and Utilization*; ACS Symposium Series 809; American Chemical Society: Washington, DC, 2001.

(24) (a) Behr, A., Ed. *Carbon Dioxide Activation by Metal Complexes*; VCH: Weinheim, 1988. (b) Walther, D.; Ruben, M.; Rau, S. *Coord. Chem. Rev.* **1999**, *182*, 67−100. (c) Yin, X.; Moss, J. R. *Coord. Chem. Rev.* **1999**, *181*, 27−59.

(25) (a) Jessop, P. G.; Ikariya, T.; Noyori, R. *Chem. Rev.* **1995**, *95*, 259−272. (b) Leitner, W. *Angew. Chem., Int. Ed. Engl.* **1995**, *34*, 2207−2221. (c) Leitner, W. *Coord. Chem. Rev.* **1996**, *153*, 257−284.

(26) Jessop, P. G.; Joo, F.; Tai, C.-C. *Coord. Chem. Rev.* **2004**, *248*, 2425−2442.

(27) Inoue, Y.; Izumida, H.; Sasaki, Y.; Hashimoto, H. *Chem. Lett.* **1976**, 863−864.

(28) Ng, S. M.; Yin, C.; Yeung, C. H.; Chan, T. C.; Lau, C. P. *Eur. J. Inorg. Chem.* **2004**. 1788−1793.

(29) (a) Jessop, P. G.; Ikariya, T.; Noyori, R. *Nature* **1994**, *368*, 231−233. (b) Munshi, P.; Main, A. D.; Linehan, J. C.; Tai, C.-C.; Jessop, P. G. *J. Am. Chem. Soc.* **2002**, *124*, 7963−7971. (c) Tai, C.-C.; Pitts, J.; Linehan, J. C.; Main, A. D.; Munshi, P.; Jessop, P. G. *Inorg. Chem.* **2002**, *41*, 1606−1614.

(30) (a) Fornika, R.; Goris, H.; Seemann, B.; Leitner, W. *J. Chem. Soc., Chem. Commun.* **1995**, 1479−1481. (b) Angermund, K.; Baumann, W.; Dinjus, E.; Fornika, R.; Gorls, H.; Kessler, M.; Kruger, C.; Leitner, W.; Lutz, F. *Chem. Eur. J.* **1997**, *3*, 755−764. (c) Leiner, W.; Dinjus, E.; Gassner, F. In *Aqueous-Phase Organometallic Catalysis, Concepts and Applications*; Cornils, B.; Herrmann, W. A., Eds.; Wiley-VCH: Weinheim, 1998; pp 486−498.

(31) (a) Joo, F.; Laurenczy, G.; Nadasdi, L.; Elek, J. *Chem. Commun.* **1999**, 971−972. (b) Laurenczy, G.; Joo, F.; Nadasdi, L. *Inorg. Chem.* **2000**, *39*, 5083−5088. (c) Elek, J.; Nadasdi, L.; Papp, G.; Laurenczy, G.; Joo, F. *Appl. Catal. A: Gen.* **2003**, *255*, 59−67. (d) Joszai, I.; Joo, F. *J. Mol. Catal. A* **2004**, *224*, 87−91.

(32) (a) Khan, M. M. T.; Halligudi, S. B.; Shukla, S. *J. Mol. Catal.* **1989**, *57*, 47−60. (b) Horvath, H.; Laurenczy, G.; Katho, A. *J. Organomet. Chem.* **2004**, *689*, 1036−1045.

(33) Tai, C.-C.; Chang, T.; Roller, B.; Jessop, P. G. *Inorg. Chem.* **2003**, *42*, 7340−7341.

(34) (a) Lubineau, A. *Chem. Ind.* (*London*) **1996**, 123−126. (b) Kuntz, E. G. *CHEMTECH* **1987**, 570−575.

(35) Cornils, B.; Herrmann, W. A. *Aqueous-Phase Organometallic Catalysis, Concepts and Applications*; Wiley-VCH: Weinheim, 1998; Chapter 1.

(36) (a) *Aqueous-Phase Organometallic Catalysis, Concepts and Applications*; Cornils, B.; Herrmann, W. A., Eds.; Wiley-VCH: Weinheim, 1998; Chapter 3. (b) Dwars, T.; Oehme, G. *Adv. Synth. Catal.* **2002**, *344*, 239−260. (c) Pinault, N.; Bruce, D. W. *Coord. Chem. Rev.* **2003**, *241*, 1−25.

(37) (a) Himeda, Y.; Onozawa-Komatsuzaki, N.; Sugihara, H.; Arakawa, H.; Kasuga, K. *Organometallics* **2004**, *23*, 1480−1483. (b) *Stud. Surf. Sci. Catal.* **2004**, *153*, 263−266. (c) Himeda, Y.; Onozawa-Komatsuzaki, N.; Sugihara, H.; Kasuga, K. *J. Photochem. Photobiol. A: Chem.* **2006**, *182*, 306−309.

(38) Himeda, Y.; Onozawa-Komatsuzaki, N.; Sugihara, H.; Kasuga, K. *J. Am. Chem. Soc.* **2005**, *127*, 13118−13119.

(39) (a) Himeda, Y.; Onozawa-Komatsuzaki, N.; Sugihara, H.; Arakawa, H.; Kasuga, K. *J. Mol. Catal. A* **2003**, *195*, 95−100. (b) Himeda, Y.; Onozawa-Komatsuzaki, N.; Sugihara, H.; Arakawa, H.; Kasuga, K. *Abstracts of Papers. The 50th Symposium on Coordination Chemistry of Japan*; Kusatsu, Japan Society of Coordination Chemistry: Okazaki, Japan, Sept. 2000; Abstract 1P3K01.

(40) Himeda, Y.; Onozawa, N.; Sugihara, H.; Arakawa, H.; Kasuga, K. Jpn. Kokai Tokkyo Koho JP 2004224715, 2004.

Scheme 1. (a) Acid−Base Equilibrium between Pyridinol and Pyridinolate. (b) Interconversion between Pyridinol and Pyridinolate Form. (c) pH Change in Solution during the Hydrogenation of Bicarbonate in Water

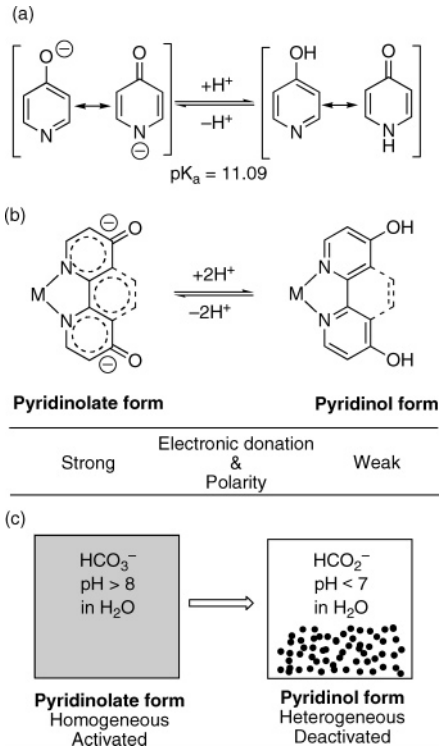

We focused on the acid−base equilibrium between pyridinol and pyridinolate (Scheme 1(a)).[41] The interconversion leads to a change in the electronic states, which is attributed to the difference between the hydroxyl in pyridinol and oxyanion in pyridinolate. According to the Hammett constant (σ_p^+),[42] the oxyanion group exhibits stronger electron-donating ability (−2.30) than that of the hydroxyl group (−0.91). Furthermore, it is known that the dipole moment of pyridone is much greater than that of pyridinol.[43] Accordingly, when pyridinol is used as a part of a complex ligand, it is expected that the interconversion provides an excellent opportunity for the catalyst properties to change significantly, namely, the electronic donation and polarity (Scheme 1(b)). Although there are interesting studies on the complexes that use the acid−base equilibrium between pyridinol and pyridinolate,[44−47] its application to a catalyst ligand have not been examined thus far.

Further, the pH of the solution changes during the reaction of CO_2 with H_2 in alkaline aqueous solution. CO_2 is hydrated almost completely to give bicarbonate in an alkaline solution under pressurized conditions.[48,49] The reaction solution changes from basic to acidic, because the hydrogenation gives formate and then formic acid after the consumption of the added base.[31d] Thus, we expect that the catalyst may transform from the homogeneous and activated pyridinolate form at the beginning of the reaction into the heterogeneous and deactivated pyridinol form at the end (Scheme 1(c)). In this study, we investigated 4,4′-dihydroxy-2,2′-bipyridine (DHBP:H_2L^1) and 4,7-dihydroxy-1,10-phenanthroline (DHPT:H_2L^2) as variable ligands for tunable catalysts.

Chart 1

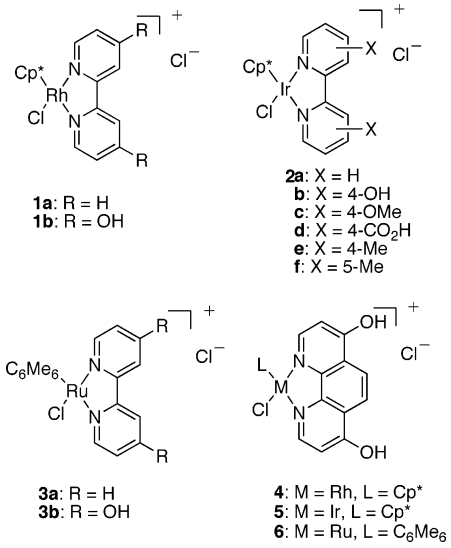

Scheme 2

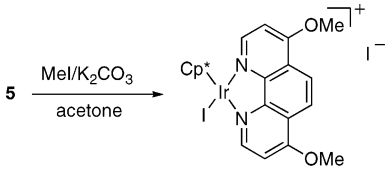

Chart 2

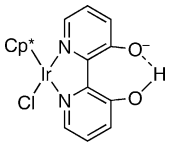

2.2. Synthesis, Characterization, and Properties. The half-sandwich Rh(III), Ir(III), and Ru(II) complexes were easily prepared by reacting $[Cp^*MCl_2]_2$ ($Cp^* = C_5Me_5$, M = Rh, Ir) or $[(C_6Me_6)RuCl_2]_2$ with the corresponding bipyridine or phenanthroline derivatives (Chart 1). Further, 4,7-dimethoxy-1,10-phenanthroline (Me_2L^2) complex **7** was prepared by the methylation of **5** (Scheme 2) because the direct alkylation of DHPT yields *N*,*O*-dialkyl derivative as the major compound.[50] In the ^1H NMR spectra, the signals for the hydroxyl protons of the DHBP and DHPT complexes in DMSO-d_6 appeared between 12 and 13 ppm as a broadened singlet, which integrated for 2H. On the other hand, complex **8** with 3,3′-dihydroxy-2,2′-bipyridine (H_2L^3) showed a broadened singlet at 18.1 ppm,

(41) (a) Albert, A.; Phillips, J. N. *J. Chem. Soc.* **1956**, 1294−1304. (b) Boga, C.; Bonamartini, A. C.; Forlani, L.; Modarelli, V.; Righi. L.; Sgarabotto, P.; Todesco, P. E. *Eur. J. Org. Chem.* **2001**, 1175−1182. (c) Tee, O. S.; Paventi, M. *Can. J. Chem.* **1983**, *61*, 2556−2562.

(42) Hansch, C.; Leo, A.; Taft, R. W. *Chem. Rev.* **1991**, *91*, 165−195.

(43) (a) Wang, J.; Boyd, R. J. *J. Phys. Chem.* **1996**, *100*, 16141−16146. (b) Gao, J.; Shao, L. *J. Phys. Chem.* **1994**, *98*, 13772−13779.

(44) Giordano, P. J.; Bock, C. R.; Wrighton, M. S. *J. Am. Chem. Soc.* **1978**, *100*, 6960−6965.

(45) Chan, C.-M.; Fung, C.-S.; Wong, K.-Y.; Lo, W. *Analyst* **1998**, *123*, 1843−1847.

(46) Price, J. M.; Xu, W.; Demas, J. N.; DeGraff, B. A. *Anal. Chem.* **1998**, *70*, 265−270.

(47) Tomon, T.; Koizumi, T.; Tanaka, K. *Eur. J. Inorg. Chem.* **2005**, 285−293.

(48) Kudo, K.; Sugita, N.; Takezaki, Y. *Nippon Kagaku Kaishi* **1977**, 302−309.

(49) The pH of an aqueous solution is dependent on the pressure of CO_2: Bonilla, R. J.; James, B. R.; Jessop, P. G. *Chem. Commun.* **2000**, 941−942.

(50) Ballesteros, P.; Claramunt, R. M.; Elguero, J. *Tetrahedron* **1987**, *43*, 2557−2564.

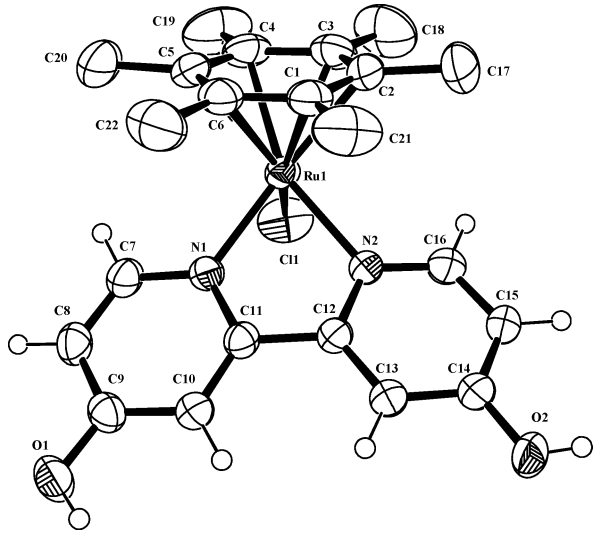

Figure 1. ORTEP view of **3b**.[67] The counteranion (Cl^-), methanol, and hydrogen atoms of η^6-C_6Me_6 are omitted for clarity.

Table 2. Crystallographic Data for 3b

formula	$C_{23}H_{30}Cl_2N_2O_3Ru$
molecular weight	554.47
T/K	296
crystal system	monoclinic
space group	$P2_1/a$ (no. 14)
a/Å	14.404 (5)
b/Å	13.017 (3)
c/Å	13.027 (4)
β/deg	101.745 (3)
V/Å^3	2391.28 (1)
Z	4
D_{calc}/g cm^{-3}	1.540
μ/cm^{-1}	9.06
radiation (λ/Å)	Mo Kα (0.7107)
R [$F^2 \geq 2\sigma(F^2)$]	0.033
R_w [$w = 1/\sigma^2(F_0)$]	0.057

Table 3. Selected Bond Lengths (Å) and Angle (deg) for 3b

Ru−N(1)	2.085(3)	Ru−N(2)	2.091(2)
Ru−C(1)	2.183(3)	Ru−C(2)	2.219(3)
Ru−C(3)	2.218(3)	Ru−C(4)	2.225(3)
Ru−C(5)	2.241(3)	Ru−C(6)	2.183(4)
O(1)−C(9)	1.328(4)	O(2)−C(14)	1.338(4)
Ru−Cl(1)	2.398(1)	N(1)−Ru−N(2)	75.9(1)

which integrated for 1H.[51] The observation and elemental analyses suggest the existence of an intramolecular O−H−O hydrogen bond in **8** (Chart 2).

A single-crystal X-ray crystallographic analysis of **3b** revealed that η_6-C_6Me_6, chlorine atoms, and two nitrogen atoms of the bipyridine ligand, existed in a distorted octahedral coordination environment (Figure 1). Crystallographic data and selected bond lengths and angle for **3b** are listed in Table 2 and 3, respectively. The structural features of **3b** are similar to those of 4,4′-dimethoxy-2,2′-bipyridine and bipyridine analogues.[52]

The complexes with bipyridine derivatives are water-soluble, whereas the complexes with unsubstituted phenanthroline are less water-soluble. On the other hand, the DHBP and DHPT complexes show the pH-dependent water solubility: highly soluble in a basic solution, but hardly soluble under acidic and neutral conditions.

2.3. Electronic Effect. The electronic effect of the substituent of a catalyst ligand on the catalytic performance has been widely investigated in the range from the electron-withdrawing nitro group to the donating amine groups.[53,54] On the basis of the theoretical study by Sakaki on the hydrogenation of CO_2 into formic acid, the strongly donating ligand would improve the catalytic efficiency.[55] First, we examined the effect of the introduction of a hydroxy group into the pyridine ring as a catalyst ligand for the hydrogenation of bicarbonate. The comparison of TON in the rhodium, iridium, and ruthenium complexes are listed in Table 4. The modification caused a considerable activation of the catalyst. In the iridium and ruthenium catalysts, the TONs of the dihydroxy complexes were 52−103 times greater than those of the unsubstituted ones. In the rhodium complexes, the rates of increase against the unsubstituted complexes were moderate (8−10 times), although the unsubstituted rhodium complexes were highest among the unsubstituted complexes.

Table 4. Substituent Effect of Ligand on TON for Hydrogenation of Bicarbonate[a]

	TON		TON	
cat.[b] L =	bpy	DHBP	phen	DHPT
Rh	216[c]	1800	220	2300
Ir	105[c]	5500	59	6100
Ru	68	4400	78[c]	5100

[a] The reactions were carried out under 4 MPa (CO_2:H_2 = 1:1) at 80 °C for 20 h in an aqueous 1 M KOH solution containing the complex (0.1 mM). [b] Catalyst: Rh = [Cp*Rh(L)Cl]Cl, Ir = [Cp*Ir(L)Cl]Cl, Ru = [(C_6Me_6)Ru(L)Cl]Cl. [c] Catalyst concentration was 0.2 mM.

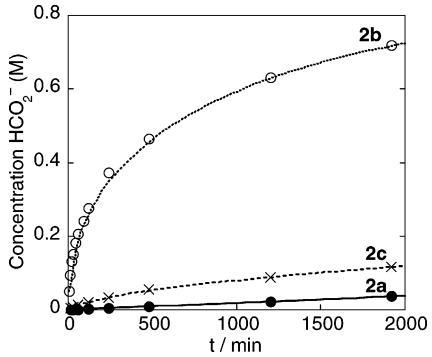

Figure 2. Time course of formate concentration for the hydrogenation of bicarbonate catalyzed by **2a**−**c** (0.2 mM) under 4 MPa (H_2:CO_2 = 1:1) at 80 °C in an aqueous 1 M KOH solution.

Next, the time courses of the formate generation were examined using the unsubstituted, dihydroxy, and dimethoxy bipyridine iridium complexes **2a**−**c** (Figure 2). The catalytic activity of **2b** was considerably greater than that of **2c**, although the σ_p^+ value of the methoxy group (−0.78) is marginally greater than that of the hydroxy group (−0.92).[42] This result suggests that the electronic effects of the substituent on **2a**−**c** are considerably different.

(51) Cargill Thompson, A. M. W.; Jeffery, J. C.; Liard, D. J.; Ward, M. D. *J. Chem. Soc., Dalton Trans.* **1996**, 879−884.

(52) (a) Hayashi, H.; Ogo, S.; Fukuzumi, S. *Chem. Commun.* **2004**, 2714−2715. (b) Ogo, S.; Abura, T.; Watanabe, Y. *Organometallics* **2002**, *21*, 2964−2969.

(53) (a) Park, S.-B.; Murata, H.; Matsumoto, H.; Nishiyama, H. *Tetrahedron: Asymmetry*, **1995**, *6*, 2487−2494. (b) Dijkstra, H. P.; Slagt, M. Q.; McDonald, A.; Kruithof, C. A.; Kreiter, R.; Mills, A. M.; Lutz, M.; Spek, A. L.; Klopper, W.; van Klink, G. P. M.; van Koten G. *Eur. J. Inorg. Chem.* **2003**, 830−838. (c) Jacobsen, E. N.; Zhang, W.; Guler, M. L. *J. Am. Chem. Soc.* **1991**, *113*, 6703−6704. (d) Constantine, R. N.; Kim, N.; Bunt, R. C. *Org. Lett.* **2003**, *5*, 2279−2282.

(54) (a) Sullivan, B. P.; Meyer, T. J. *Organometallics* **1986**, *5*, 1500−1502. (b) Ribeiro, P. E. A.; Donnici, C. L.; dos Santos, E. N. *J. Organomet. Chem.* **2006**, *691*, 2037−2043. (c) McFarland, J. M.; Francis, M. B. *J. Am. Chem. Soc.* **2005**, *127*, 13490−13491. (d) Aubel, P. G.; Khokhar, S. S.; Driessen, W. L.; Challa, G.; Reedijk. J. *J. Mol. Catal. A* **2001**, *175*, 27−31. (e) ten Brink, G. J.; Arends, I.; Hoogenraad, M.; Verspui, G.; Sheldon, R. A. *Adv. Synth. Catal.* **2003**, *345*, 1341−1352.

(55) Ohnishi, Y.; Matsunaga, T.; Nakao, Y.; Sato, H.; Sakaki, S. *J. Am. Chem. Soc.* **2005**, *127*, 4021−4032.

Table 5. Hydrogenation of Bicarbonate Catalyzed by Iridium Complexes[a]

entry	catalyst/concn (mM)	initial TOF (h^{-1})	TON
1	**2a**/0.2	6	105
2	**2c**/0.2	9	137
3	**2d**/0.2	13	128
4	**2e**/0.2	82[b]	444
5	**2b**/0.05	7960[b]	6770
6	**7**/0.1	140	1170
7	**2f**/0.2	5	64
8	**8**/0.1	(6)[c]	150

[a] The reaction was carried out under 4 MPa (CO_2:H_2 = 1:1) at 80 °C for 20 h in an aqueous 1 M KOH solution. [b] The initial TOFs were calculated by nonlinear least-squares fits of the experimental data from the initial part of the reaction. See ref 48. [c] Average TOFs in parentheses.

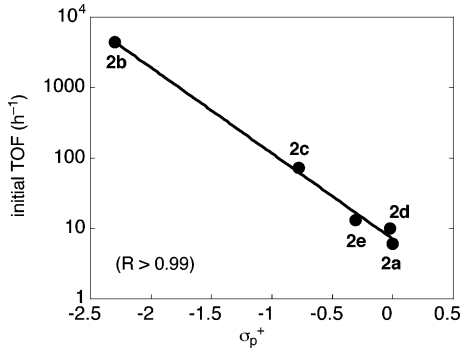

Figure 3. Hammett plot of log(initial TOF) vs the σ_p^+ value of substituent in **2a**−**e**. The reaction was carried out with **2a**−**e** (0.05−0.2 mM) under 4 MPa (CO_2:H_2 = 1:1) at 80 °C in an aqueous 1 M KOH solution.

Therefore, we systematically examined the electronic effect using a series of iridium complexes [Cp*Ir(4,4′-X_2-2,2′-bpy)Cl]Cl **2a**−**e** on the basis of the Hammett rule. The TONs and initial TOFs are summarized in Table 5. It should be noted that the deprotonation of the phenolic hydroxyl group on **2b** and the carboxyl group on **2d** occurs under basic reaction conditions. Thus, the σ_p^+ values for **2b** and **2d** are regarded to be −2.30 and −0.02, which corresponds to the oxyanion (O^-) and carboxylato (CO_2^-) values, respectively.[42] The Hammett plot of log(initial TOF) vs the σ_p^+ value of X in **2**, as shown in Figure 3, exhibits a good correlation ($R > 0.99$). Likewise, a similar reactivity trend (H < OMe < OH) was observed for the series of phenanthroline complexes ([Cp*Ir(phen)Cl]Cl, **5**, and **7** (entry 6)). These results are in good agreement with Sakaki's theoretical prediction[55] and Jessop's experimental results[29c] for the catalytic hydrogenation of CO_2.

The effects of the position of the substituent on the catalytic activity were examined. As expected, the complex with 5,5′-dimethyl-2,2′-bipyridine **2f** was not activated (entry 7). Surprisingly, no significant activation was observed in **8**, although one negative charge existed on the ligand (entry 8). One possible explanation could be that the resonance structures of 3-hydroxypyridine cannot increase the π-electron density on the nitrogen atoms. This hypothesis is consistent with the data reported for nucleophilicity of the nitrogen atom in the 3- and 4-hydroxypyridine anions.[56]

Table 6 summarized the results by using the DHBP and DHPT complexes. The iridium complexes were superior to the corresponding rhodium analogues (entries 1 vs 3 and 2 vs 7). In the former, unprecedented high activities (TOF of 42 000 h^{-1} (entry 5) and TON of 220 000 (entry 11)) were obtained under 6 MPa at 120 °C in a highly diluted solution of the catalyst ($< 2 \times 10^{-6}$ M). Furthermore, hydrogenation proceeded under ambient pressure at 60 °C (entries 6 and 9) and even at 30 °C (entry 10). To the best of our knowledge, there is only one other report on homogeneous catalytic hydrogenation of CO_2 that occurs under ambient pressure at room temperature.[30c]

The arene−ruthenium complexes **3b** and **6** yielded higher concentrations of formate as compared to the iridium complexes, although their TOF and TON values were moderate (entries 12−15). The concentrations increased steadily with increasing pressure from 1.08 M at 2 MPa to 1.54 M at 6 MPa. An increase in the reaction temperature consequently increased the TOF without degradation in the product yield (Figure S1 in the Supporting Information). However, under ambient pressure, a small amount of formate was generated (TOF = 1.8 at 60 °C).

Interestingly, we observed no significant decomposition of the formate as the reverse reaction, which is sometimes a problem in the hydrogenation of CO_2 and bicarbonate after pressure release. This suggests that the catalyst activity decreases considerably at the end of the reaction: the catalyst may change from the activated pyridinolate form into the deactivated pyridinol form.

Consequently, we found highly efficient catalysts for the hydrogenation of bicarbonate attributed to the electronic effect of the strong electron-donating oxyanion group, which was generated from pyridinol ligands such as DHBP or DHPT. The catalytic efficiency (TOF, TON, and concentration of formate) is strongly affected by the central metals. On the other hand, the difference between the effects of the DHBP and DHPT ligands on the catalytic efficiency is relatively small. To the best of our knowledge, this is the first example applicable to an oxyanion on a catalyst ligand.

2.4. Water Solubility. The pH-dependent water solubility of the complexes may be attributed to the acidic phenolic group. The absorption spectra of the complexes depend on the pH due to the acid−base equilibrium (Figure S2 in the Supporting Information).[44] In fact, the fully protonated complexes were recovered by acidification of the alkaline solution of the deprotonated complexes.[57] The concentrations of the residual complexes decreased in the order Rh ≈ Ru > Ir, and the DHPT complexes exhibit a lower solubility than the DHBP complexes. The solutes may be aqua complexes generated by aquation of the chloro complexes.[58] Interestingly, the complexes recovered from the pyridinolate form of **5** at around weakly acidic conditions were pH-dependent mixtures (^{1}H NMR). The mixtures of the complexes were only partially soluble in DMSO-d_6, although these were easily transformed into the pyridinolate form in D_2O/KOD. The mixtures may consist of monoprotonated and fully protonated complexes.

We examined the solubility of iridium complexes **2b** and **5** in formate solutions, which are similar to the reaction conditions. The alkaline solution of iridium complexes was added to 1 M formate solution at various pH values. The color of the solution (ca. 20 ppm of iridium) immediately changed from pale yellow to deep yellow. After allowing it to stand overnight, a yellow solid precipitated and the solution became colorless. The iridium concentrations of the filtrates were measured with ICP-MS (Figure 4). In weakly acidic conditions, the solubilities are considerably low. In particular, the iridium concentration of **5** was as low as 0.12 ppm at pH values of 4.5−5.0, which is at

(56) Deady, L. W.; Finlayson, W. L.; Potts, C. H. *Aust. J. Chem.* **1977**, *30*, 1349−1352.

(57) The recovered complexes were confirmed by ^{1}H NMR and elemental analysis.

(58) (a) Dadci, L.; Elias, H.; Frey, U.; Hornig, A.; Koelle, U.; Merbach, A. E.; Paulus, H.; Schneider, J. S. *Inorg. Chem.* **1995**, *34*, 306−315. (b) Bennett, M. A.; Ennett, J. P. *Organometallics* **1984**, *3*, 1365−1374.

Table 6. Hydrogenation of Bicarbonate Using the Complexes Having DHBP or DHPT Ligand[a]

entry	catalyst/concn (μM)	temp (°C)	P (MPa)	time (h)	initial TOF[b] (h^{-1})	TON	final concn of formate (M)
1	**1b**/100	80	4	12	790	1800	0.18
2	**4**/100	80	4	32	270	2400	0.24
3	**2b**/100	80	4	140	4000	8000	0.80
4	**2b**/20	120	6	32	41000	33500	0.67
5	**2b**/0.5	120	6	57	42000	190000	0.095
6	**2b**/200[c]	60	0.1	50	33	376	0.075
7	**5**/100	80	4	116	3000	7300	0.73
8	**5**/20	120	6	32	35000	26000	0.52
9	**5**/200[c]	60	0.1	50	32	444	0.089
10	**5**/200[c]	30	0.1	30	3.5	81	0.016
11	**5**/2	120	6	48	33000	222000	0.44
12	**3b**/100[d]	120	6	8	4400	13620	1.36
13	**6**/100[d]	80	4	165	370	12500	1.25
14	**6**/100[d]	120	6	24	3600	15400	1.54
15	**6**/100[d]	100	2	92	600	10800	1.08

[a] The reaction was carried out in an aqueous 1 M KOH solution under the desired CO_2:H_2 (1:1) pressure. [b] The initial TOFs were calculated by nonlinear least-squares fits of the experimental data from the initial part of the reaction. See ref 48. [c] The reaction was carried out in an aqueous 0.1 M K_2CO_3 solution. [d] The reaction was carried out in an aqueous 2 M KOH solution.

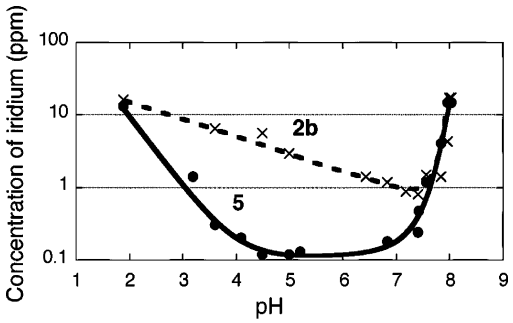

Figure 4. Iridium concentration in an aqueous 1 M formate solution.

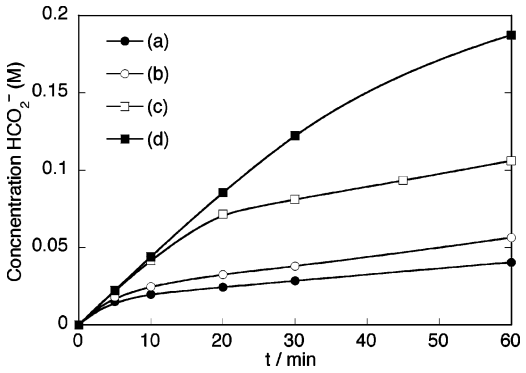

Figure 5. Time course of formate concentration for the hydrogenation of bicarbonate catalyzed by **5** (0.05 mM) under 6 MPa (CO_2:H_2 = 1:1) at 60 °C in (a) 0.1 M, (b) 0.2 M, (c) 0.5 M, and (d) 1.0 M aqueous KOH solutions.

almost one-seventh that of **2b** (0.80 ppm at a pH of 7.4). The recovered solids were mixtures of hydride complexes, which may consist of monoprotonated and fully protonated complexes. On the other hand, at a pH of 3.5 and below the solubility of both the complexes increased, and gas evolution was observed probably due to the decomposition of formic acid. The results suggest that water-soluble aqua complexes are generated.[59] The precipitation of rhodium and ruthenium complexes was not observed under these conditions. This may be due to the instability of the hydride complexes (*vide infra*).

It was found that the water solubilities of the complexes are dependent on the pH of the solution as well as the central metals. The differences between the solubility of the DHBP and DHPT ligands in formate solution are significant, although the difference in their catalytic activity is marginal. Among these complexes, the iridium−DHPT complex **5** will be favorable for catalyst recovery and catalytic efficiency.

2.5 Optimization of Catalysis. The above-mentioned results encouraged us to try to optimize the catalysis. First, we investigated the influence of the KOH concentration on the catalytic performance using **5**. Figure 5 shows the time course of the formate concentration in various KOH concentrations during an initial period of 60 min using **5** (0.05 mM) at 6 MPa of H_2:CO_2 (1:1) at 60 °C. In all the reactions, the maximum TOFs (ca. 5000 h^{-1}) were observed at the beginning of the reaction. After 5 min, the reaction rate decreased drastically in 0.1 and 0.2 M KOH solutions. In 1.0 M KOH solution, the rate was steady up to 30 min, and it then decreased gradually.

On the other hand, the yields of the formate, namely, the pH of final reaction solution, affected the catalyst solubility at the end of the reaction (Table 7). When the reaction was carried out in 0.5 M solutions for 72 h, the added KOH could not be consumed; therefore, 0.61 ppm of iridium remained in the solution. By using 0.2 M solutions, the concentration of the formate exceeded that of the added KOH after 48 h and therefore iridium leaching decreased to 0.19 ppm. In particular, in 0.1 M KOH solutions, the colorless filtrate (pH = 5.5) was found to contain only 0.11 ppm of iridium, which was 1.2% of the loaded catalyst. Furthermore, by evaporation of the filtrate and drying under vacuum at 100 °C, pure potassium formate was obtained (>98% pure).[60] These results imply the possibility of catalyst recycling in the conversion of CO_2 into formate without waste generation.

Table 7. Influence of KOH Concentration on the Reaction Performance Using 5[a]

KOH (M)	time (h)	leaching [Ir] (ppm)[b]	final concn of formate (M)	pH of final solution
0.5	72	0.61	0.476	7.5
0.2	48	0.19	0.201	6.8
0.1	20	0.11	0.105	5.5

[a] The reaction was carried out using **5** (0.05 mM) under 6 MPa (CO_2:H_2 = 1:1) at 60 °C. [b] The iridium concentration was measured by ICPMS analysis.

Then, the reusability of **5** was examined in the batchwise cycle (Table 8). The above-mentioned recovered catalyst

(59) (a) Abura, T.; Ogo, S.; Watanabe, Y.; Fukuzumi, S. *J. Am. Chem. Soc.* **2003**, *125*, 4149−4154. (b) Ogo, S.; Uehara, K.; Abura, T.; Watanabe, Y.; Fukuzumi, S. *Organometallics* **2004**, *23*, 3047−3052.

(60) Mp 166−169 °C (Aldrich catalog gives 165−168 °C). Anal. Calcd for CHO_2K: C, 14.28; H, 1.20. Found: C, 14.25; H, 1.16. Bicarbonate was not detected by ^{13}C NMR analysis, in which the spectral signal-to-noise (S/N) ratio was over 50. The produced formic acid may decompose during drying.

Table 8. Batchwise Catalyst Recycling in the Conversion of CO_2 into Formate Using 5

cycle	loaded/recovered [Ir] (ppm)[a]	recovery efficiency (%)	leaching [Ir] (ppm)[a]	final concn of formate (M)[b]
1	9.0	−	0.11	0.105
2	8.4	93	0.22	0.104
3	7.7	92	0.42	0.103
4	7.0	91	0.61	0.103

[a] The iridium concentration was measured by ICP-MS analysis. [b] For all the four cycles, no bicarbonate was detected.

Scheme 3. Recycling System of the Conversion of CO_2/H_2 and KOH into HCO_2K Using 5 in Water

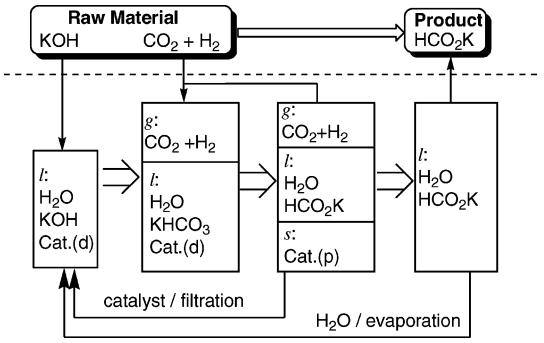

g: gas phase, *l*: liquid phase, *s*: solid phase, cat.(d): deprotonated form, cat.(p): protonated form.

precursor was dissolved in a 0.1 M degassed aqueous KOH solution, in which ICP-MS analysis of the solution indicated that 93% iridium was recovered (the loss of iridium was due to the sampling for assay (2%) and handling losses). While the recovered catalyst retained high catalytic activity for all the four cycles, leaching increased and recovery decreased with an increase in the recycling of the catalyst. The batch experiments require a careful handling of the reaction solutions that contain air-sensitive active species, but some exposure to air cannot be avoided. This problem can be overcome if a continuous closed system or an integrated membrane reactor is used. By using NaOH as the base, a similar result was obtained by the same procedure. However, when the reaction was carried out at 80 °C for 10 h, iridium leaching increased up to 0.9 ppm and catalyst recovery decreased to 75%. It appears that the thermal stress and exposure to air lead to an increase in catalyst leaching.

It was found that the reusability of **5** was achieved by the self-precipitation at the end of the reaction. Furthermore, it is interesting to note that the three components (i.e., catalyst, product, and solvent) can be easily separated by using conventional filtration and evaporation without waste generation (Scheme 3). This catalytic system combines the advantages of both homogeneous (i.e., high catalytic performance) and heterogeneous (i.e., the simplicity of catalyst separation) catalyzes.

2.6. Mechanism. The identification and/or isolation of intermediates were conducted in each reaction step. The deprotonated complexes [Cp*Ir(L^1)Cl]K (**9**) and [(C_6Me_6)Ru(L^1)Cl]K (**10**) were isolated from an alkaline ethanolic solution (Scheme 4). The ^{1}H NMR signals for the aromatic protons of **9** were shifted upfield, and the ^{13}C NMR signal for the carbons attached to oxygen was shifted downfield compared to those of pyridinol form **5** (Table 9). The ^{1}H NMR spectrum of **9** in D_2O was nearly identical with that of **5** in KOD/D_2O.

We examined the generation of hydride complexes from the pyridinolate form in KOD/D_2O with pressurized H_2, as monitored by ^{1}H NMR. The iridium hydride complexes [Cp*Ir−H(L^1)]$^-$ **11** and [Cp*Ir−H(L^2)]$^-$ **12** were quantitatively generated under H_2 pressure (>0.4 MPa). In the ruthenium complexes, hydride complex [(C_6Me_6)Ru−H(L^1)]$^-$ **13** or [(C_6Me_6)Ru−H(L^2)]$^-$ **14** was observed as a mixture with the pyridinolate form of **3b** or **6**, respectively, in which the ratios depended on the H_2 pressure. The hydride complexes slowly reverted into their original form under an atmosphere of H_2. However, rhodium hydrides were not detected and the complexes were decomposed. It can be observed that the ease in the generation and stability of hydride complexes increases in the order Rh ≪ Ru ≪ Ir. The addition of $KHCO_3$ to the aqueous solution of hydride complex **12** led to the production of formate in 90% yield in an atmosphere of H_2. However, no formate was generated in the reaction with K_2CO_3.

Scheme 4

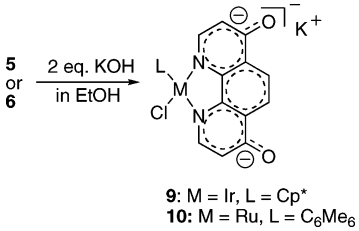

9: M = Ir, L = Cp*
10: M = Ru, L = C_6Me_6

Table 9. ^{1}H and ^{13}C NMR Spectral Data for Iridium Complexes 5, 9, and 12

	^{1}H NMR/ppm				^{13}C NMR/ppm
complex/solvent	**H**-2,9	**H**-5,6	**H**-3,8	**Ir-H**	**C**-4,7
5/DMSO	8.94	8.20	7.44	−	161.8
9/DMSO	7.86	7.62	6.22	−	175.4
5/KOD/D_2O	8.55	7.94	6.78	−	174.5
12/KOD/D_2O	8.40	7.92	6.75	−11.10	175.7

The solubility behavior of **5** during the course of the reaction was visually observed by using a glass reactor containing 0.1 M KOH aqueous solution (50 mL) of **5** (1.6 mg). Complex **5** was completely soluble in the KOH solution with pressurized CO_2, in which CO_2 exists as bicarbonate.[48] When the reactor was recharged with 3 MPa of H_2:CO_2 (1:1) at 60 °C, the pale yellow solution turned orange, which may indicate the formation of a hydride complex.[61] After 30 min, a yellow precipitate was formed. After a further 2.5 h, the resulting suspension was filtered through a PTFE filter to give a clear pale yellow filtrate and yellow precipitate. The filtrate (pH = 7.9) was found to contain 0.05 M of formate (50% conversion) and 1.0 ppm of iridium (ca. 10% of the loaded iridium). The precipitate was readily converted to a pyridinolate form by the addition of an aqueous base (^{1}H NMR).

These observations suggest the plausible mechanism depicted in Scheme 5. The catalyst precursor as the pyridinol form (**PX**: X = Cl) was deprotonated and transformed into the pyridinolate form (**DX**) under an alkaline solution. In the presence of H_2, a deprotonated hydride complex (**DH**) was formed, which probably is the actual catalyst. The actual substrate presumably is bicarbonate, excluding carbonate.[27,31,48] It is reasonable to assume that bicarbonate is inserted into the metal−hydride bond and then generate the formato intermediate with the release of a hydroxide ion, as suggested by Joo and co-workers in their study.[31b]

During the course of the reaction, the acidification due to formate generation may cause the transformation from the pyridinolate form (**D**) into the monoprotonated (**M**), or fully protonated form (**P**). Consequently, decreases in the water

(61) Sandrini, D.; Maestri, M.; Ziessel, R. *Inorg. Chim. Acta* **1989**, *163*, 177−180.

Scheme 5. Proposed Mechanism for Hydrogenation of Bicarbonate to Formate

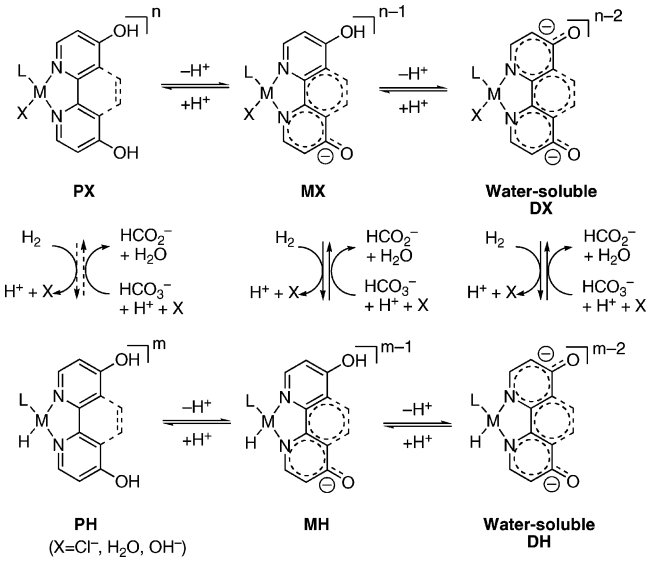

solubility and catalytic activity can be attributed to this phenomenon. In particular, iridium−DHPT complexes, whose solubility is negligible in weak acidic formate conditions, could be recovered at the end of the reaction.

3. Conclusion

A highly efficient and environmentally benign CO_2 conversion process was found by using DHBP and DHPT as the catalyst ligands. We concluded that these significant features are attributed to the simultaneous catalyst tuning of activity and water solubility by an acid−base equilibrium between pyridinol and pyridinolate. In particular, it was found that the oxyanion generated from the phenolic hydroxy group plays significant roles in catalytic activity and water solubility. For example, using the iridium catalysts gave a TOF of up to 42 000 h^{-1} and TON of up to 222 000. This is the first example of an oxyanion applicable to a catalyst ligand. Furthermore, the iridium−DHPT complex was precipitated spontaneously at the end of the reaction, in which iridium leaching was found to be 0.11 ppm (1.2% of the loaded catalyst) and the added base was completely consumed. The recovered catalyst can be recycled for four cycles with a high catalytic activity. The catalyst, product, and solvent could be easily separated by conventional filtration and evaporation without waste generation. The catalyst combines the advantages of both homogeneous and heterogeneous catalyzes. The catalyst design concept may hold significantly broader implications for the design of new homogeneous catalysts for catalyst activation, introduction of water solubility, and catalyst recovery.

4. Experimental Section

General Considerations. All manipulations were carried out under an argon atmosphere using standard Schlenk techniques or in a glovebox. All aqueous solutions were degassed prior to use. ^1H and ^{13}C NMR spectra were recorded on a Varian INOVA 400 spectrometer using tetramethylsilane (TMS) or sodium 3-(trimethylsilyl)-1-propanesulfonate (DSS) as an internal standard. FAB MS spectra were recorded on a JEOL JMS-DX303. Elemental analyses were carried out on an Eager 200 instrument. FT-IR spectra were recorded on a Perkin-Elmer Spectrum One spectrometer. UV spectra were recorded on a JASCO-550 spectrometer. The pH values were measured on an Orion Model 290A pH meter with a glass electrode after calibration to standard buffer solutions. The formate concentrations were monitored by an HPLC on an anion-exclusion column (Tosoh TSKgel SCX(H^+)) with an aqueous phosphate solution (20 mM) as an eluent and a UV detector (λ = 210 nm).[62] Inductively coupled plasma mass spectrometry (ICP-MS) analyses of iridium ions were carried out using a Shimadzu ICPM-8500 at Shimadzu Techno-Research Inc. (Sample Nos. KC-22060, 24050, 24912, 27922, and 28328). Research grade CO_2 (>99.999%), H_2 (>99.9999%), and CO_2/H_2 (>99.999%) were used. $[Cp^*RhCl_2]_2$, $[Cp^*IrCl_2]_2$, $[(C_6Me_6)RuCl_2]_2$, 4,4′-dicarboxy-2,2′-bipyridine, 4,4′-dimethyl-2,2′-bipyridine, 5,5′-dimethyl-2,2′-bipyridine, 4,4′-dimethoxy-2,2′-bipyridine and 3,3′-dihydroxy-2,2′-bipyridine were commercially available from either Aldrich or Tokyo Kasei. A 4,7-dihydroxy-1,10-phenanthroline, which was purchased from Aldrich, was washed with water and then filtered to remove water-soluble inorganic impurities prior to use. The 4,4′-dihydroxy-2,2′-bipyridine,[63] **1a**,[64] **2a**,[65] **2d**,[65] **3a**,[58a] $[Cp^*Rh(phen)Cl]Cl$,[64] $[Cp^*Ir(phen)Cl]Cl$,[65] and $[(C_6Me_6)Ru(phen)Cl]Cl$[66] were prepared according to the literature procedures.

Representative Procedure for the Preparation of 4,4′-Dihydroxy-2,2′-bipyridine Complexes (Method A): 4,4′-Dihydroxy-2,2′-bipyridine Rhodium Complex $[Cp^*Rh(H_2L^1)Cl]Cl$ (1b). A DMF solution (10 mL) of $[Cp^*RhCl_2]_2$ (309 mg, 0.50 mmol) and 4,4′-dihydroxy-2,2′-bipyridine (190 mg, 1.01 mmol) was stirred at 40 °C for 12 h. The solvent was reduced in vacuo. The residues were dissolved in methanol, and the suspension was filtered off. The volume of the filtrate was reduced to ∼5 mL in vacuo, and ethyl acetate was added to precipitate a pale yellow solid. The crude complex was purified by recrystallization from ethanol−AcOEt to give **1b** (403 mg, 81%) as yellow crystals: IR (KBr) 1620, 1570, 1493, 1468, 1346, 1257, 1217, 1023; ^1H NMR (DMSO-d_6) δ 12.1 (bs, 2 H), 8.57 (d, J = 6.5 Hz, 2 H), 7.83 (d, J = 2.7 Hz, 2 H), 7.21 (dd, J = 6.5, 2.7 Hz, 2 H), 1.62 (s, 15 H); ^{13}C NMR (DMSO-d_6) δ 165.27, 153.53, 150.76, 113.69, 109.12, 93.89 (d, J_{Rh}−C = 8.4 Hz), 6.45; ^1H NMR (D_2O/KOD) δ 8.28 (d, J = 6.6 Hz, 2 H), 7.14 (d, J = 2.6 Hz, 2 H), 6.69 (dd, J = 2.6, 6.6 Hz, 2 H), 1.57 (s, 15 H); ^{13}C NMR (D_2O/KOD) δ 178.77, 159.01, 153.21, 121.46, 115.88, 96.00 (d, J_{Rh}−C = 7.6 Hz), 10.26; UV λ_{max} (MeOH) 373 (2 800), 236 nm (45 500); Anal. Calcd for $C_{20}H_{23}Cl_2N_2O_2Rh\cdot 1/2H_2O$: C, 47.45; H, 4.78; N, 5.53. Found: C, 47.77; H, 5.03; N, 5.22; FABMS m/z 461 $[M - Cl]^+$.

A 6 N HCl aqueous solution (0.4 mL) was added to the 1 N NaOH aqueous solution (1 mL) of **1b** (33 mg) to precipitate the yellow solid (23 mg). Anal. Calcd for $C_{20}H_{23}Cl_2N_2O_2Rh\cdot 1/2H_2O$: C, 47.45; H, 4.78; N, 5.53. Found: C, 47.42; H, 4.91; N, 5.21.

4,4′-Dihydroxy-2,2′-bipyridine iridium complex $[Cp^*Ir(H_2L^1)Cl]Cl$ (2b) was prepared from $[Cp^*IrCl_2]_2$ (400 mg, 0.50 mmol) and 4,4′-dihydroxy-2,2′-bipyridine (190 mg, 1.01 mmol) according to the procedure described for Method A to afford **2b** (484 mg, 85%) as yellow crystals: dec >250 °C; IR (KBr) 1622, 1572, 1495, 1475, 1451, 1312, 1262, 1220; ^1H NMR (DMSO-d_6) δ 12.0 (bs, 2 H), 8.56 (d, J = 6.5 Hz, 2 H), 7.87 (d, J = 2.5 Hz, 2 H), 7.19 (dd, J = 2.5, 6.5 Hz, 2 H), 1.62 (s, 15 H); ^{13}C NMR (DMSO-d_6) δ 167.77, 157.12, 153.09, 116.65, 111.97, 88.42, 8.82; ^1H NMR (D_2O/KOD) δ 8.26 (d, J = 6.6 Hz, 2 H), 7.14 (d, J = 2.7 Hz, 2 H), 6.63 (dd, J = 2.7, 6.6 Hz, 2 H), 1.57 (s, 15 H); ^{13}C NMR (D_2O/ KOD) δ 178.63, 159.80, 152.94, 121.48, 115.94, 87.50, 10.23; UV λ_{max} (MeOH) 342 (4 900), 236 nm (27 900); Anal. Calcd for $C_{20}H_{23}$-

(62) Komatsuzaki, N.; Himeda, Y.; Hirose, T.; Sugihara, H.; Kasuga, K. *Bull. Chem. Soc. Jpn.* **1999**, *72*, 725−731.
(63) Hong, Y.-R.; Gorman, C. B. *J. Org. Chem.* **2003**, *68*, 9019−9025.
(64) Kolle, U.; Kang, B.-S.; Infelta, P.; Comte, P.; Gratzel, M. *Chem. Ber.* **1989**, *122*, 1869−1880.
(65) Ziessel, R. *J. Am. Chem. Soc.* **1993**, *115*, 118−127.
(66) Canivet, J.; Karmazin-Brelot, L.; Suss-Fink, G. J. *J. Organomet. Chem.* **2005**, *690*, 3202−3211.

$Cl_2IrN_2O_2$: C, 40.96; H, 3.95; N, 4.78. Found: C, 40.56; H, 3.86; N, 4.55; FABMS *m*/*z* 551 $[M - Cl]^+$.

A 6 N HCl aqueous solution (0.4 mL) was added to the 1 N NaOH aqueous solution (1 mL) of **2b** (33 mg) to precipitate the yellow solid (28 mg). Anal. Calcd for $C_{20}H_{23}Cl_2IrN_2O_2 \cdot 1/2H_2O$: C, 40.34; H, 4.06; N, 4.70. Found: C, 40.23; H, 4.09; N, 4.46.

4,4′-Dimethoxy-2,2′-bipyridine Iridium Complex [Cp*Ir-(Me_2L^1)Cl]Cl (2c). A methanol solution (20 mL) of $[Cp^*IrCl_2]_2$ (200 mg, 0.25 mmol) and 4,4′-dimethoxy-2,2′-bipyridine (110 mg, 0.51 mmol) was stirred at 40 °C for 12 h. The solvent was removed *in vacuo*, and the residue was dissolved in a minimum amount of acetone. Addition of diethyl ether gave a pale yellow precipitate **2c** (293 mg, 95%), which was collected, washed with ether, and dried *in vacuo*. An analytical sample was obtained by chromatography on a Sephadex LH-20 (Pharmacia Fine Chemicals) column with methanol as the eluent: dec >200 °C; IR (KBr) 1619, 1560, 1496, 1339, 1257, 1232; ^{1}H NMR (DMSO-d_6) δ 8.73 (d, J = 6.6 Hz, 2 H), 8.37 (d, J = 2.7 Hz, 2 H), 7.40 (dd, J = 6.6, 2.7 Hz, 2 H), 4.09 (s, 6 H), 1.63 (s, 15 H); ^{13}C NMR (DMSO-d_6) δ 168.33, 156.91, 153.21, 115.21, 111.04, 88.66, 57.67, 8.65; Anal. Calcd for $C_{22}H_{27}Cl_2IrN_2O_2$: C, 42.99; H, 4.43; N, 4.56. Found: C, 42.86; H, 4.79; N, 4.17; FABMS *m*/*z* 579 $[M - Cl]^+$.

4,4′-Dimethyl-2,2′-bipyridine iridium complex [Cp*Ir(4,4′-Me_2-2,2′-bpy)Cl]Cl (2e). A methanol solution (20 mL) of $[Cp^*IrCl_2]_2$ (200 mg, 0.25 mmol) and 4,4′-dimethyl-2,2′-bipyridine (94 mg, 0.51 mmol) was stirred at 40 °C for 12 h. The residues were dissolved in acetonitrile, and the suspension was filtered off. The volume of the filtrate was reduced to ~5 mL in vacuo, and ethyl acetate was added to precipitate **2e** as a pale yellow solid (263 mg, 90%). An analytical sample was obtained by recrystallization from acetonitrile/ethyl acetate: IR (KBr) 1621, 1453, 1028; ^{1}H NMR (DMSO-d_6) δ 8.80 (d, J = 5.9 Hz, 2 H), 8.64 (s, 2 H), 7.68 (bd, J = 5.9 Hz, 2 H), 2.63 (s, 6 H), 1.64 (s, 15 H); ^{13}C NMR (DMSO-d_6) δ 152.57, 150.39, 149.22, 127.44, 122.62, 86.73, 18.79, 6.17; Anal. Calcd for $C_{22}H_{27}Cl_2IrN_2 \cdot H_2O$: C, 44.00; H, 4.87; N, 4.66. Found: C, 44.10; H, 4.83; N, 4.62; FABMS *m*/*z* 547 $[M - Cl]^+$.

5,5′-Dimethyl-2,2′-bipyridine iridium complex [Cp*Ir(5,5′-Me_2-2,2′-bpy)Cl]Cl (2f). A methanol solution (20 mL) of $[Cp^*IrCl_2]_2$ (200 mg, 0.25 mmol) and 5,5′-dimethyl-2,2′-bipyridine (94 mg, 0.51 mmol) was stirred at 40 °C for 12 h. The solution was concentrated to ~5 mL, and diethyl ether was added to precipitate **2f** as a pale yellow solid (270 mg, 92%). An analytical sample was obtained by recrystallization from methanol/ethyl acetate: IR (KBr) 1478, 1386, 1246; ^{1}H NMR (DMSO-d_6) δ 8.70 (bs, 2 H), 8.63 (d, J = 8.2 Hz, 2 H), 8.15 (bd, J = 8.2 Hz, 2 H), 2.56 (s, 6 H), 1.66 (s, 15 H); ^{13}C NMR (DMSO-d_6) δ150.67, 149.24, 138.85, 137,20, 121.21, 87.00, 15.92, 6.20; Anal. Calcd for $C_{22}H_{27}Cl_2IrN_2$: C, 45.36; H, 4.67; N, 4.81. Found: C, 45.21; H, 4.57; N, 4.71; FABMS *m*/*z* 547 $[M - Cl]^+$.

4,4′-Dihydroxy-2,2′-bipyridine ruthenium complex [(C_6Me_6)-Ru(H_2L^1)Cl]Cl (3b) was prepared from $[(C_6Me_6)RuCl_2]_2$ (335 mg, 0.50 mmol) and 4,4′-dihydroxy-2,2′-bipyridine (190 mg, 1.01 mmol) according to the procedure described for Method A to afford **3b** (415 mg, 79%) as yellow crystals: dec >250 °C; IR (KBr) 1619, 1570, 1491, 1447, 1312, 1262, 1221, 1024; ^{1}H NMR (DMSO-d_6) δ 12.1 (bs, 2 H), 8.51 (d, J = 6.5 Hz, 2 H), 7.76 (d, J = 2.7 Hz, 2 H), 7.17 (dd, J = 6.5, 2.7 Hz, 2 H), 2.00 (s, 18 H); ^{13}C NMR (DMSO-d_6) δ 167.18, 156.05, 154.57, 115.65, 111.33, 94.65, 15.53; ^{1}H NMR (D_2O/KOD) δ 8.17 (d, J = 6.7 Hz, 2 H), 7.05 (d, J = 2.6 Hz, 2 H), 6.63 (dd, J = 2.6, 6.7 Hz, 2 H), 1.98 (s, 18 H); ^{13}C NMR (D_2O/KOD) δ 178.55, 159.07, 154.98, 120.94, 115.59, 95.14, 17.25; UV λ_{max} (MeOH) 342 (3 500), 253 nm (23 200); Anal. Calcd for $C_{22}H_{26}Cl_2N_2O_2Ru$: C, 50.58; H, 5.02; N, 5.36. Found: C, 50.24; H, 5.24; N, 5.11; FABMS *m*/*z* 487 $[M - Cl]^+$.

A 6 N HCl aqueous solution (0.4 mL) was added to the 1 N NaOH aqueous solution (1 mL) of **3b** (33 mg) to precipitate the yellow solid (18 mg). Anal. Calcd for $C_{22}H_{26}Cl_2N_2O_2Ru \cdot H_2O$: C, 48.89; H, 5.22; N, 5.18. Found: C, 49.04; H, 5.11; N, 5.09.

Representative Procedure for the Preparation of 4,7-Dihydroxy-1,10-phenanthroline Iridium Complexes: [Cp*Ir(H_2L^2)-Cl]Cl (5). A DMF solution (10 mL) of $[Cp^*IrCl_2]_2$ (400 mg, 0.50 mmol) and 4,7-dihydroxy-1,10-phenanthroline (250 mg, 1.18 mmol) was stirred at 80 °C for 6 h. After cooling, the yellow precipitate was filtered off. The filtrate remained amount of desired product, but it was difficult to separate. The yellow solids were dissolved in ethanol, and the suspension was filtered off. The volume of the filtrate was reduced to ~10 mL in vacuo, and ether was added to precipitate **5** as a pale yellow solid (360 mg, 59%). An analytical sample was obtained by chromatography on a Sephadex LH-20 (Pharmacia Fine Chemicals) column with ethanol as the eluent. IR (Nujol) 2669 (O−H), 2587 (O−H), 1608, 1583, 1542, 1226; ^{1}H NMR (DMSO-d_6) δ 13.2 (bs, 2 H), 8.94 (d, J = 6.3 Hz, 2 H), 8.20 (s, 2 H), 7.44 (d, J = 6.3 Hz, 2 H), 1.69 (s, 15 H); ^{13}C NMR (DMSO-d_6) δ 161.80, 150.37, 145.89, 120.19, 118.30, 109.09, 85.71, 6.32; ^{1}H NMR (D_2O/KOD) δ 8.55 (d, J = 6.5 Hz, 2 H), 7.94 (s, 2 H), 6.78 (d, J = 6.5 Hz, 2 H), 1.63 (s, 15 H); ^{13}C NMR (D_2O/KOD) δ 174.53, 150.51, 149.45, 126.99, 119.17, 113.78, 85.03, 8.11; UV λ_{max} (MeOH) 357 (11 200), 243 nm (25 300); Anal. Calcd for $C_{22}H_{23}Cl_2IrN_2O_2$: C, 43.28; H, 3.80; N, 4.59. Found: C, 43.20; H, 3.90; N, 4.38; FABMS *m*/*z* 575 $[M - Cl]^+$.

A 6 N HCl aqueous solution (0.4 mL) was added to the 1 N NaOH aqueous solution (1 mL) of **5** (33 mg) to precipitate the yellow solid (28 mg). Anal. Calcd for $C_{22}H_{23}Cl_2IrN_2O_2 \cdot H_2O$: C, 42.04; H, 4.01; N, 4.46. Found: C, 42.03; H, 4.09; N, 4.25.

4,7-Dihydroxy-1,10-phenanthroline Rhodium Complexes: [Cp*Rh(H_2L^2)Cl]Cl (4). Yield 37%; IR (Nujol) 2669 (O−H), 2590 (O−H), 1603, 1583, 1540, 1225; ^{1}H NMR (DMSO-d_6) δ 13.0 (bs, 2 H), 8.93 (d, J = 6.2 Hz, 2 H), 8.16 (s, 2 H), 7.41 (d, J = 6.2 Hz, 2 H), 1.69 (s, 15 H); ^{13}C NMR (DMSO-d_6) δ 162.45, 150.34, 144.59, 120.39, 117.69, 109.12, 93.68 (d, J_{Rh}−C = 8.4 Hz), 6.62; ^{1}H NMR (D_2O/KOD) δ 8.51 (d, J = 6.4 Hz, 2 H), 7.91 (s, 2 H), 6.80 (d, J = 6.4 Hz, 2 H), 1.97 (s, 15 H); ^{13}C NMR (D_2O/KOD) δ 176.61, 153.04, 150.49, 129.02, 120.97, 116.12, 95.56 (d, J_{Rh}−C = 7.6 Hz), 10.28; UV λ_{max} (MeOH) 353 (10 800), 232 nm (28 800); Anal. Calcd for $C_{22}H_{23}Cl_2N_2O_2Rh$: C, 50.69; H, 4.45; N, 5.37. Found: C, 50.35; H, 4.44; N, 5.45; FABMS *m*/*z* 485 $[M - Cl]^+$.

A 6 N HCl aqueous solution (0.4 mL) was added to the 1 N NaOH aqueous solution (1 mL) of **4** (33 mg) to precipitate the yellow solid (27 mg). Anal. Calcd for $C_{22}H_{23}Cl_2N_2O_2Rh \cdot H_2O$: C, 49.00; H, 4.67; N, 5.19. Found: C, 49.02; H, 4.74; N, 5.12.

4,7-Dihydroxy-1,10-phenanthroline Ruthenium Complexes: [(C_6Me_6)Ru(H_2L^2)Cl]Cl (6). An analytical sample was obtained by recrystallization from addition of HCl to an aqueous alkaline solution of **6**: Yield 41%; IR (Nujol) 2672 (O−H), 2593 (O−H), 1606, 1583, 1512, 1222; ^{1}H NMR (DMSO-d_6) δ 13.2 (bs, 2 H), 8.88 (d, J = 6.3 Hz, 2 H), 8.11 (s, 2 H), 7.38 (d, J = 6.2 Hz, 2 H), 2.07 (s, 18 H); ^{13}C NMR (DMSO-d_6) δ 161.08, 151.99, 144.57, 119.56, 117.88, 108.67, 92.06, 13.31; ^{1}H NMR (D_2O/KOD) δ 8.56 (d, J = 6.4 Hz, 2 H), 7.92 (s, 2 H), 6.84 (d, J = 6.4 Hz, 2 H), 2.02 (s, 18 H); ^{13}C NMR (D_2O/KOD) δ 176.34, 154.80, 150.67, 128.68, 120.88, 115.64, 94.82, 17.31; UV λ_{max} (MeOH) 349 (10 400), 247 nm (24 900); Anal. Calcd for $C_{24}H_{26}Cl_2N_2O_2Ru \cdot H_2O$: C, 51.07; H, 5.00; N, 4.96. Found: C, 50.72; H, 4.79; N, 4.91; FABMS *m*/*z* 511 $[M - Cl]^+$.

A 6 N HCl aqueous solution (0.4 mL) was added to the 1 N NaOH aqueous solution (1 mL) of **6** (33 mg) to precipitate the yellow solid (28 mg). Anal. Calcd for $C_{24}H_{26}Cl_2N_2O_2Ru \cdot H_2O$: C, 51.07; H, 5.00; N, 4.96. Found: C, 51.26; H, 4.98; N, 4.90.

4,7-Dimethoxy-1,10-phenanthroline Iridium Complex [Cp*Ir-(Me_2L^2)I]I (7). To a stirred suspension of **5** (61 mg, 0.10 mmol) and K_2CO_3 (200 mg) in acetone (50 mL) was added iodomethane (130 μL, 2.0 mmol). The suspension was heated to 70 °C for 12 h

with vigorous stirring. After cooling, the solid was filtered off. The filtrate was concentrated in vacuo. The resulting yellow solids were dissolved in a minimum amount of methanol, and then diethyl ether was added to precipitate a pale yellow solid. The solid was purified by chromatography on Sephadex LH-20 eluting with methanol to give **7** (61 mg, 78%) as a pale yellow solid: IR (KBr) 1607, 1578, 1526, 1301; ^{1}H NMR (DMSO-d_6) δ 9.16 (d, J = 6.5 Hz, 2 H), 8.30 (s, 2 H), 7.64 (d, J = 6.5 Hz, 2 H), 4.30 (s, 6 H), 1.79 (s, 15 H); ^{13}C NMR (DMSO-d_6) δ 164.18, 155.14, 146.81, 122.69, 121.34, 108.42, 89.82, 58.27, 9.53; Anal. Calcd for $C_{24}H_{27}I_2IrN_2O_2$: C, 35.09; H, 3.31; N, 3.41. Found: C, 35.25; H, 3.55; N, 3.21; FABMS m/z 695 $[M - I]^+$.

[Cp*Ir(HL^3)Cl] (8). Following the procedure for preparation of **2b**, $[Cp^*IrCl_2]_2$ (100 mg, 0.125 mmol) was allowed to reacted with 3,3′-dihydroxy-2,2′-bipyridine (48 mg, 0.255 mmol) to give complex **8** as a yellow solid (100 mg, 72%). Further purification was carried out by recrystallization from dichloromethane−EtOAc. IR (KBr) 1645, 1582, 1260; ^{1}H NMR (DMSO-d_6) δ 18.1 (bs, 1 H, O−H−O), 8.06 (dd, J = 5.2, 1.3 Hz, 2 H), 7.26 (dd, J = 8.4, 5.2 Hz, 2 H), 7.06 (dd, J = 8.4, 1.3 Hz, 2 H), 1.56 (s, 15 H); ^{1}H NMR (D_2O/KOD) δ 8.33 (d, J = 5.6 Hz, 2 H), 7.42 (dd, J = 8.4, 5.6 Hz, 2 H), 7.31 (d, J = 8.4 Hz, 2 H), 1.59 (s, 15 H); ^{13}C NMR (DMSO-d_6) δ 159.06, 143.74, 137.80, 127.14, 124.99, 86.16, 6.04; Anal. Calcd for $C_{20}H_{22}ClIrN_2O_2$: C, 43.67; H, 4.03; N, 5.09. Found: C, 43.60; H, 3.86; N, 4.86; FABMS m/z 551 $[M + H]^+$, 515 $[M - Cl]^+$.

[Cp*Ir(L^2)Cl]K (**9**). To a solution of **5** (62 mg, 0.1 mmol) in absolute ethanol (10 mL) was added a 0.5 M potassium hydroxide in ethanol (400 μL, 0.2 mmol). After stirring for 10 min, anhydrous diethyl ether (100 mL) was added to precipitate the pale yellow solid. The solid was filtered off and washed with diethyl ether. The crude product was recrystallized from methanol/diethyl ether to give **9** (23 mg, 37%) as a yellow hygroscopic solid. IR (KBr) 1602, 1559, 1497; ^{1}H NMR (DMSO-d_6) δ 7.86 (d, J = 6.9 Hz, 2 H), 7.62 (s, 2 H), 6.22 (d, J = 6.9 Hz, 2 H), 1.69 (s, 15 H); ^{13}C NMR (DMSO-d_6) δ 175.40, 149.34, 149.22, 129.44, 118.46, 115.31, 95.05, 8.69; ^{1}H NMR (D_2O) δ 8.56 (d, J = 6.5 Hz, 2 H), 7.94 (s, 2 H), 6.78 (d, J = 6.5 Hz, 2 H), 1.63 (s, 15 H); Anal. Calcd for $C_{22}H_{21}ClIrKN_2O_2 \cdot H_2O$: C, 41.93; H, 3.68; N, 4.45. Found: C, 42.02; H, 3.89; N, 4.20; FABMS (glycerol) m/z 613 $[M + H]^+$, 575 $[M - K + 2H]^+$, 539 $[M - K - Cl + H]^+$.

[(C$_6$Me$_6$)Ru(L^2)Cl]K (**10**). Following the procedure for preparation of **9**, **6** (55 mg, 0.1 mmol) was converted to **10** (19 mg, 35%): IR (KBr) 1599, 1551, 1492; ^{1}H NMR (DMSO-d_6) δ 7.80 (d, J = 7.1 Hz, 2 H), 7.59 (s, 2 H), 6.26 (d, J = 7.1 Hz, 2 H), 2.07 (s, 18 H); ^{13}C NMR (DMSO-d_6) δ 175.47, 151.11, 148.78, 129.58, 117.96, 115.49, 101.99, 16.02; ^{1}H NMR (D_2O) δ 8.71 (d, J = 6.4 Hz, 2 H), 7.89 (s, 2 H), 6.82 (d, J = 6.4 Hz, 2 H), 2.11 (s, 18 H); FABMS (NBA) m/z 548 $[M + H]^+$, 511 $[M - K + 2H]^+$, 475 $[M - K - Cl + H]^+$. This complex gave no satisfactory elemental analysis due to hygroscopic.

[Cp*IrH(L^1)]$^-$ (**11**). Complex **2b** (2 mg) was dissolved in 5 mL of D_2O/KOD (5 mL). The solution was allowed to stand under 2 MPa of H_2 for 4 days. ^{1}H NMR (D_2O/KOD) δ 8.15 (d, J = 6.6 Hz, 2 H), 7.15 (d, J = 2.7 Hz, 2 H), 6.58 (dd, J = 6.6, 2.7 Hz, 2 H), 1.75 (s, 15 H), −11.09 (s, 1 H, Ir−*H*); ^{13}C NMR (D_2O/KOD) δ 177.67, 159.96, 154.23, 121.10, 116.07, 91.13, 11.13.

[Cp*IrH(L^2)]$^-$ (**12**). Complex **5** (2 mg) was dissolved in 5 mL of D_2O/KOD (5 mL). The solution was allowed to stir under 0.4 MPa of H_2 for 4 days. ^{1}H NMR (D_2O/KOD) δ 8.40 (d, J = 6.5 Hz, 2 H), 7.92 (s, 2 H), 6.75 (d, J = 6.5 Hz, 2 H), 1.69 (s, 15 H), −11.10 (s, 1 H, Ir−*H*); ^{13}C NMR (D_2O/KOD) δ 175.70, 153.56, 152.08, 129.47, 121.31, 115.59, 90.71, 11.03.

[(C$_6$Me$_6$)RuH(L^1)]$^-$ (**13**). Complex **3b** (2 mg) was dissolved in 5 mL of D_2O/ KOD (5 mL). The solution was allowed to stand under 3 MPa of H_2 for 4 days to give ca. 2:3 mixture of **13** and the pyridinolate form of **3b**; ^{1}H NMR (D_2O/KOD) δ 8.15 (d, J = 6.7 Hz, 2 × 3/5H), 7.83 (d, J = 6.5 Hz, 2 × 2/5H), 7.05 (d, J = 2.6 Hz, 2 × 3/5H), 7.03 (d, J = 2.8 Hz, 2 × 2/5H), 6.63 (dd, J = 2.6, 6.7 Hz, 2 × 3/5H), 6.49 (dd, J = 6.5, 2.8 Hz, 2 × 2/5H), 2.03 (s, 18 × 2/5H), 1.95 (s, 18 × 3/5H), −7.46 (s, 1 × 2/5H, Ru−*H*). The reaction was carried out under 1 MPa of H_2 for 5 day to give ca. 2:5 mixture of **13** and the pyridinolate form of **3b**.

[(C$_6$Me$_6$)RuH(L^2)]$^-$ (**14**). Complex **6** (2 mg) was dissolved in 5 mL of D_2O/ KOD (5 mL). The solution was allowed to stand under 3 MPa of H_2 for 4 days to give ca. 3:2 mixture of **14** and the pyridinolate form of **6**; ^{1}H NMR (D_2O/KOD) δ 8.49 (d, J = 6.4 Hz, 2 × 2/5H), 8.12 (dd, J = 6.5, 2.8 Hz, 2 × 3/5H), 7.90 (s, 2 × 2/ 5H), 7.83 (s, 2 × 3/5H), 6.84 (d, J = 6.4 Hz, 2 × 2/5H), 6.66 (d, J = 6.5 Hz, 2 × 3/ 5H), 2.02 (s, 18 × 3/5H), 1.98 (s, 18 × 2/5H), −7.58 (s, 1 × 3/5H, Ru−*H*). The reaction was carried out under 1 MPa of H_2 for 5 day to give ca. 1:1 mixture of **14** and the pyridinolate form of **6**.

Procedure for Catalytic Hydrogenation of Bicarbonate under Pressurized Conditions. A degassed aqueous KOH solution (50 mL) of the complex was saturated with CO_2 in a 100 mL stainless steel reactor equipped with a sampling device. The reactor was heated and then repressurized to the desired CO_2:H_2 (1:1) pressure. At appropriate intervals, samples were removed and analyzed by HPLC. The initial TOFs were calculated using nonlinear least-squares fitting of the experimental data obtained from the initial part of the reaction.[48]

Procedure for Catalytic Hydrogenation of Bicarbonate under Ambient Conditions. A degassed aqueous KCO_3 solution (20 mL) of the complex (4.0 mmol) was saturated with CO_2 at ambient pressure. The solution was heated and vigorously stirred under an atmosphere of CO_2:H_2 (1:1). All gases were passed through an oxygen trap prior to use. At appropriate intervals, samples were removed and analyzed by HPLC.

Reaction of 11 with KHCO$_3$. A degassed solution of **5** (15 mg, 24.5 μmol) and K_3PO_4 (150 mg) in 10 mL of D_2O was pressurized with 4 MPa of H_2 at room temperature for 72 h to generate **11**. Excess $KHCO_3$ was added to this solution, and the reaction mixture was allowed to stand under atmospheric pressure of H_2 at room temperature for 4 h in NMR tube to yield a 2.4 mM of formate solution (yield >90%), which was analyzed by means of HPLC.

Measurement of Iridium Leaching in an Aqueous Formate. To a 1 M format solution (15 mL) with various pH values was added a 100 μL of KOH (0.1−0.05 M) aqueous solution of the complex (15 mM). The obtained solutions or suspensions were allowed to stand at room temperature for 24 h. These were filtered to give the solution, whose iridium concentration was measured by ICP-MS.

UV Studies of Acid−Base Equilibrium. To a 50 mM sodium phosphate buffer (3.9 mL) adjusted to the appropriate pH was added a 100 μL of 2 mM solution of hydroxy complex in MeOH (the fully protonated hydroxy complex is insoluble in water). The UV−vis spectrum of each solution was measured after reading the pH value.

Procedure for Catalyst Recycling. A degassed aqueous 0.1 M KOH solution (50 mL) of **5** (1.5 mg, 2.5 μmol) was saturated with CO_2 in a 100 mL stainless steel reactor. The reactor was heated at 60 °C and then repressurized under 6 MPa of CO_2:H_2 (1:1). After stirring for 20 h, the solution was allowed to stir under a reduced pressure for 2 h at rt and was then cooled to 0 °C in a refrigerator for 12 h. The suspension was filtered through a 0.2 μm PTFE filter membrane to recover the catalyst precursor. In order to avoid contamination, the recycling experiments were conducted using the above-mentioned apparatus. The reaction mixtures (0.5 mL × 2) were sampled at the beginning and end of each run for the assay of the concentration of iridium and formate, respectively.

X-ray Crystallographic Analysis. Measurements were made on a Mac Science MXC18 diffractometer with graphite-monochromated Mo Kα (λ = 0.7107 Å). All the calculations were performed

using the teXsan crystallographic software package from Molecular Structure Corp. A hydrogen atom attached O(3) of methanol was not found in D-Fourier. The figure was generated with ORTEP-3 for Windows.[67]

Acknowledgment. We thank Dr. Midori Goto, Technical Service Center, AIST, for the X-ray structure determinations. This work was supported by the COE development program of Ministry of Education, Culture, Sports, Science and Technology of Japan.

(67) ORTEP-3 for Windows: Farrugia, L. J. *J. Appl. Crystallogr.* **1997**, *30*, 565.

Supporting Information Available: ^{1}H NMR spectra for **10**−**14**, figures, and crystallographic information (CIF) for **3b**. This material is available free of charge via the Internet at http://pubs.acs.org.

OM060899E